Available online at www.sciencedirect.com
SCIENCE DIRECT®
Journal of Colloid and Interface Science 295 (2006) 279–290
JOURNAL OF Colloid and Interface Science
www.elsevier.com/locate/jcis

Sedimentation of a concentrated dispersion of composite colloidal particles

Eric Lee, Kuang-Ting Chou, Jyh-Ping Hsu *

Department of Chemical Engineering, National Taiwan University, Taipei, Taiwan 10617

Received 19 March 2005; accepted 2 August 2005

Available online 31 August 2005

Abstract

The sedimentation of a concentrated spherical dispersion of composite particles, where a particle comprises a rigid core and a membrane layer containing fixed charge, is investigated theoretically. The dispersion is simulated by a unit cell model, and a pseudo-spectral method based on Chebyshev polynomials is adopted to solve the problem numerically. The influences of the thickness of double layer, the concentration of particles, the surface potential of the rigid core of a particle, and the amount of fixed charge in the membrane layer on both the sedimentation potential and the sedimentation velocity are discussed. Several interesting results are observed; for example, depending upon the charged conditions on the rigid core and in the membrane layer of a particle, the sedimentation potential might have both a local maximum and a local minimum and the sedimentation velocity can have a local minimum as the thickness of double layer varies. Also, the sedimentation velocity can have a local maximum as the surface potential varies. We show that the sedimentation potential increases with the concentration of particles. The relation between the sedimentation velocity and the concentration of particles, however, depends upon the thickness of double layer.
© 2005 Elsevier Inc. All rights reserved.

Keywords: Sedimentation; Concentrated spherical dispersion; Composite particle; Double-layer polarization; Double-layer overlapping

1. Introduction

Sedimentation, the falling of dispersed particles driven by gravity, has various applications in practice. For instance, it can be used as a solid–liquid separation tool in both laboratory and industrial scales. Alternatively, the physical properties such as the density of the dispersed particles can be estimated through measuring their rate of sedimentation. For a charged, spherical colloidal particle, the original symmetric electric double layer surrounding it may become asymmetric when it sediments; counterions are accumulated in the downstream region and there is an excess of coions in the upstream region. An induced electric field is established, and, regardless of the sign of the surface charge, this induced electric field has the effect of hindering the sedimentation of a particle [1–7]. Under general conditions, the analysis of the sedimentation of colloidal particles involves solving coupled, nonlinear electrokinetic equations, and only if drastic assumptions are made, deriving an analytical solution is almost impossible. For example, assuming low zeta potential and thin electrical double layer, that is, the interaction between adjacent double layers is negligible, Levine et al. [8] derived an analytical expression for both the sedimentation potential and sedimentation velocity for a concentrated suspension of spherical colloidal particles. Under the same condition, Ohshima [9] derived a simple expression for the sedimentation potential.

In practice, sedimentation of colloidal particles is often conducted under conditions where the concentration of particles is appreciable. Since the movement of a particle will be influenced unavoidably both electrically and hydrodynamically by neighboring particles, it is expected that the sedimentation behavior of a dispersion of particles be different from that of an isolated particle. Considerable efforts

* Corresponding author. Fax: +886 2 23623040.
E-mail address: jphsu@ntu.edu.tw (J.-P. Hsu).

0021-9797/$ – see front matter © 2005 Elsevier Inc. All rights reserved.
doi:10.1016/j.jcis.2005.08.009

have been made to estimate the effect of the concentration of rigid particles on their sedimentation behaviors under various conditions [8–12]. These analyses are common in that the difficulty of solving a many-body problem is circumvented by adopting Kuwabara's unit cell model [13], where a spherical dispersion is mimicked by a representative cell comprising a particle and a concentric spherical liquid shell possessing the properties of the dispersion medium. This model, while is an idealized one, provides a concise description of a complicated system, and is capable of, at least qualitatively, predicting its behavior.

Similarly to rigid particles, nonrigid particles also play an important role in colloidal science. Typical example includes biocolloids such as biological cells and microorganisms and particles covered by a membrane or surfactant layer. These particles are characterized by having an ion-penetrable surface layer, which is capable of influencing appreciably the transport behavior of a particle both in a flow field and in an electric field. Theoretical analysis on the sedimentation of composite particles became active recently, and some analytical results based on low electric potentials were derived [14,15]. As stated above, the effect of double-layer polarization is one of the key components in sedimentation. Since this effect is most important when the surface potential of a particle is sufficiently high and the thickness of double layer surrounding it is comparable to its linear size [16,17], an analysis based on these conditions is highly desirable.

In this study, previous analyses on the sedimentation of concentrated rigid colloidal particles are extended to the case of composite particles where a particle comprises a rigid core and a membrane layer carrying fixed charge, which arises from the dissociation of the functional groups. A rigid particle is a special case of composite particle since the former can be recovered as a limiting case of the latter by letting the thickness of the membrane layer approaches zero. We consider the case where both the concentration of the dispersed phase and the thickness of the double layer surrounding a particle can be arbitrary. The latter implies that the interaction between neighboring double layers needs to be taken into account.

2. Theory

Let us consider the sedimentation of a concentrated dispersion of composite, spherical particles of radius $(a + d)$, a and d being respectively the radius of the rigid core of a particle and the thickness of its membrane layer. Both the surface of the rigid core and the membrane layer are charged. Referring to Fig. 1, the system under consideration is simulated by a representative cell of radius c which comprises a particle and a concentric liquid shell of thickness $(c - b)$. This so-called unit cell model [18] mimics the spherical dispersion with the volume fraction of particles measured by $H = (b/c)^3$. A $z_1 : z_2$ electrolyte is present in the liquid phase, z_1 and z_2 being respectively the valences of cations and anions with $z_2 = -\alpha z_1$. Let **U** be the sedimentation velocity of the particle, **g** be the gravitational acceleration, and **E** be an induced electric field arising from the sedimentation of the particle. As shown in Fig. 1, the spherical coordinates (r, θ, φ) are adopted with its origin located at the center of the particle. We assume that the liquid phase is an incompressible Newtonian fluid with constant physical properties, the flow of liquid phase is in the creeping flow regime, and the sedimentation reaches a quasi-steady state. Under these conditions, the governing equations of the present problem are essentially the same as those for the corresponding electrophoresis problem [18]. The scaled governing equations and the associated boundary conditions are summarized in Appendix A.

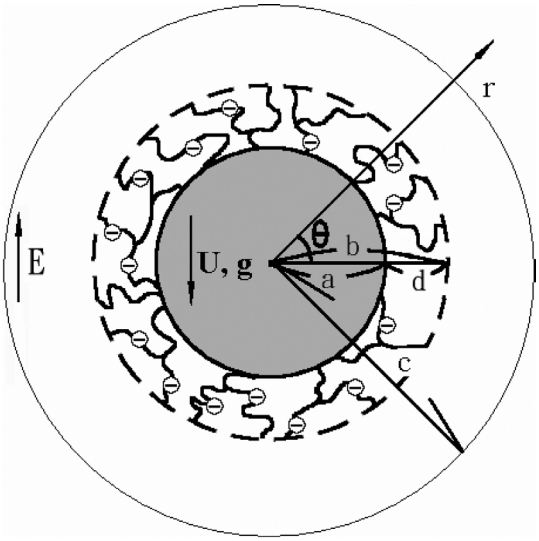

Fig. 1. Schematic representation of the sedimentation problem considered where a concentrated spherical dispersion of particles, each of them comprises a rigid core of radius a and an ion-penetrable membrane layer of thickness d, sediments in the gravitation field. The surface of the rigid core of a particle is positively charged and the membrane layer carries fixed charge. The system is simulated by a represented cell of radius c, which composed of a particle of radius b $(= a + d)$ and a concentric liquid shell of thickness $c - b$. The spherical coordinates are chosen with the origin located at the center of the particle, **U** and **g** are the sedimentation velocity and the gravitational acceleration, **E** is the induced electric field, and r and θ are respectively the radial distance and the azimuthally angle of the spherical coordinates.

2.1. Sedimentation potential

For the present case, the sedimentation of a particle leads to a polarized double layer; an excess amount of cations are accumulated in the double layer beneath the particle and an excess amount of anions in the double layer above it. This yields an induced electric field, which is in the opposite direction as that of sedimentation, and the corresponding electrical potential is called the sedimentation potential. For convenience, the scaled sedimentation potential $E_z^*/U^* = [E_z/(\zeta_a/a)]/[U/(\varepsilon\zeta_a^2/\eta a)] = \varepsilon E_z \zeta_a / U\eta$ is used in subse-

quent discussions. $E_Z^* = E_Z/(\zeta_a/a)$, where E_Z is the magnitude of the induced electric field and ζ_a is the surface potential on the rigid core of a particle. $U^* = U/(\varepsilon\zeta_a^2/\eta a)$, U is the magnitude of $\mathbf{U}$, ε and η are respectively the dielectric constant and the viscosity of the liquid phase. The sedimentation potential can be evaluated from a current balance, that is, the current arises from the sedimentation of a particle is balanced by that arises from the induced electric field [18]. The current $\mathbf{i}$ can be expressed as

$$\mathbf{i} = \sum_j z_j e n_j \mathbf{v}_j, \tag{1}$$

where e is the elementary charge and n_j and $\mathbf{v}_j$ are respectively the number concentration and the velocity of jth ionic species. At steady state, the net current across any plane perpendicular to the gravitational field should vanish. Applying this condition to $\theta = \pi/2$ yields

$$\begin{aligned}\langle i\rangle = 0 &= 2\pi \int_a^c r i_\theta \,\mathrm{d}r\big|_{\theta=\pi/2} \\ &= 2\pi \int_a^c r\left[\sum_{j=1}^{2} z_j e n_j v_{j\theta}\right]\mathrm{d}r\big|_{\theta=\pi/2}, \quad j = 1, 2,\end{aligned} \tag{2}$$

where subscript θ denotes the θ-component of a physical quantity. $\mathbf{v}_j$ and the bulk liquid velocity $\mathbf{v}$ are related by

$$\mathbf{v}_j = \mathbf{v} - D_j\left(\frac{z_j e}{kT}\nabla\phi + \frac{\nabla n_j}{n_j}\right), \tag{3}$$

where D_j is the diffusion coefficient of ionic species j, k and T are respectively the Boltzmann constant and the absolute temperature, ϕ is the electrical potential, and ∇ is the gradient operator. For simplicity, we assume that the diffusion coefficients in and out of the membrane layer are the same. Substituting this expression into Eq. (1) gives

$$\begin{aligned}\mathbf{i} = {}& \frac{\varepsilon^3\phi_r^2}{\eta a^3}\left(\frac{kT}{z_1 e}\right)^3 \frac{(\kappa a)^2}{(1+\alpha)} \\ &\times \left\{\left[\exp\left(-\phi_r\phi_1^*\right) - \exp\left(\alpha\phi_r\phi_1^*\right)\right]\mathbf{v}^* \right. \\ &+ \frac{1}{\phi_r}\left[\frac{1}{\mathrm{Pe}_1}\exp\left(-\phi_r\phi_1^*\right)\nabla^* g_1^* \right. \\ &\left.\left. + \frac{\alpha}{\mathrm{Pe}_2}\exp\left(\alpha\phi_r\phi_1^*\right)\nabla^* g_2^*\right]\right\},\end{aligned} \tag{4}$$

where $\kappa^{-1} = [\varepsilon kT/\sum n_{j0}(ez_j)^2]^{1/2}$, $\phi_r = z_1 e\zeta_a/kT$, n_{j0} and Pe_j are respectively the bulk number concentration and the electric Peclet number of the jth ionic species. The scaled gradient operator ∇^*, the scaled functions ϕ_1^*, g_1^*, and g_2^*, and the scaled velocity $\mathbf{v}^*$ are defined in our previous work [18]. The θ-component of the current $\mathbf{i}$, i_θ, is

$$\begin{aligned}i_\theta = {}& \frac{\varepsilon^3\phi_r^2}{\eta a^3}\left(\frac{kT}{z_1 e}\right)^3 \frac{(\kappa a)^2}{(1+\alpha)} \\ &\times \left\{\left[\exp\left(-\phi_r\phi_1^*\right) - \exp\left(\alpha\phi_r\phi_1^*\right)\right]\frac{\mathrm{d}\Psi}{\mathrm{d}r^*} \right. \\ &- \frac{1}{\phi_r}\left[\frac{1}{\mathrm{Pe}_1}\exp\left(-\phi_r\phi_1^*\right)G_1^* \right. \\ &\left.\left. \times \frac{\alpha}{\mathrm{Pe}_2}\exp\left(\alpha\phi_r\phi_1^*\right)G_2^*\right]\frac{\sin\theta}{r^*}\right\},\end{aligned} \tag{5}$$

where $r^* = r/a$ is the scaled radial distance, Ψ is the stream function, and the scaled functions G_1^* and G_2^* are defined in our previous work [18]. This expression can be rewritten as

$$i_\theta = I_a I_\theta(r^*)\frac{\sin\theta}{r^*}, \tag{6}$$

where

$$I_a = \frac{\varepsilon^3\phi_r^2}{\eta a^3}\left(\frac{kT}{z_1 e}\right)^3 \frac{(\kappa a)^2}{(1+\alpha)}, \tag{7}$$

$$\begin{aligned}I_\theta = {}& \left\{\left[\exp\left(-\phi_r\phi_1^*\right) - \exp\left(\alpha\phi_r\phi_1^*\right)\right]\frac{\mathrm{d}\Psi}{\mathrm{d}r^*} \right. \\ &\left. - \frac{1}{\phi_r}\left[\frac{1}{\mathrm{Pe}_1}\exp\left(-\phi_r\phi_1^*\right) + G_1^*\frac{\alpha}{\mathrm{Pe}_2}\exp\left(\alpha\phi_r\phi_1^*\right)G_2^*\right]\right\}.\end{aligned} \tag{8}$$

Substituting Eq. (8) into Eq. (2) yields

$$\langle i\rangle = 0 = 2\pi a^2 I_a \int_1^{c/a} I_\theta(r^*)\,\mathrm{d}r^*. \tag{9}$$

Similarly to the treatment for the corresponding electrophoresis problem [19], the present problem is divided into two subproblems. In the first problem a particle is moving with constant velocity $\mathbf{U}$ in the absence of the induced electric field. In this case, the average current is $\langle i\rangle_1 = \delta U^*$. In the second problem, the particle is remained fixed when the induced electric field is present. In this case, the average current is $\langle i\rangle_2 = \beta E_z^*$. Since the net current across the plane $\theta = \pi/2$ vanishes, $\langle i\rangle = \langle i\rangle_1 + \langle i\rangle_2 = 0$ and, therefore, the scaled sedimentation potential is

$$\frac{E_z^*}{U^*} = -\frac{\delta}{\beta}. \tag{10}$$

2.2. Sedimentation velocity

The evaluation of the sedimentation velocity is based on that the total force acting on a particle in the z-direction vanishes. The forces involved include the electric force, F_{Ez}, the hydrodynamic drag force, F_{Dz}, and the gravitational force, F_g. These forces can be expressed as [20,21]

$$F_{Ez} = \frac{4}{3}\pi\varepsilon\zeta_a^2\left(r^{*2}\left(\frac{\mathrm{d}\phi_1^*}{\mathrm{d}r^*}\right)\left(\frac{\mathrm{d}\Phi_2}{\mathrm{d}r^*}\right) - 2r^*\left(\frac{\mathrm{d}\phi_1^*}{\mathrm{d}r^*}\right)\Phi_2\right)_{r^*=b/a}$$
$$= \frac{4}{3}\pi\varepsilon\zeta_a^2 F_{Ez}^*, \tag{11}$$

$$F_{Dz} = \frac{4}{3}\pi\varepsilon\zeta_a^2\left[r^{*2}\frac{\mathrm{d}}{\mathrm{d}r^*}(D^2\Psi) - 2r^*(D^2\Psi)\right]_{r^*=b/a}$$
$$+ \frac{4}{3}\pi\varepsilon\zeta_a^2\frac{(\kappa a)^2}{(1+\alpha)\phi_r}$$
$$\times\left\{r^{*2}\left[\exp\left(-\phi_r\phi_1^*\right) - \exp\left(\alpha\phi_r\phi_1^*\right)\right]\Phi_2\right\}_{r^*=b/a}$$
$$= \frac{4}{3}\pi\varepsilon\zeta_a^2\left(F_{Dhz}^* + F_{DEez}^*\right) = \frac{4}{3}\pi\varepsilon\zeta_a^2 F_{Dz}^*, \tag{12}$$

$$F_g = -\frac{4}{3}\pi a^3(\rho_p - \rho_f)g - V_s(\rho_s - \rho_f)g, \tag{13}$$

with

$$F_{Ez}^* = \left(r^{*2}\left(\frac{\mathrm{d}\phi_1^*}{\mathrm{d}r^*}\right)\left(\frac{\mathrm{d}\Phi_2}{\mathrm{d}r^*}\right) - 2r^*\left(\frac{\mathrm{d}\phi_1^*}{\mathrm{d}r^*}\right)\Phi_2\right)_{r^*=b/a}, \tag{14}$$

$$F_{Dhz}^* = \left[r^{*2}\frac{\mathrm{d}}{\mathrm{d}r^*}(D^2\Psi) - 2r^*(D^2\Psi)\right]_{r^*=b/a}, \tag{15}$$

$$F_{Dez}^* = \frac{(\kappa a)^2}{(1+\alpha)\phi_r}\left\{r^{*2}\left[\exp\left(-\phi_r\phi_1^*\right)\right.\right.$$
$$\left.\left. - \exp\left(\alpha\phi_r\phi_1^*\right)\right]\Phi_2\right\}_{r^*=b/a}. \tag{16}$$

In these expressions, ρ_f, ρ_p, and ρ_s are respectively the densities of the fluid, rigid core of particle, and the membrane layer of particle, the operator D is defined in Appendix A, and the function Φ_2 is defined in our previous work [18]. The total force acting on a particle vanishes when it reaches the terminal velocity, that is, $F_{Dz} + F_{Ez} + F_g = 0$, or

$$\frac{4}{3}\pi\varepsilon\zeta_a^2\left(F_{Ez}^* + F_{Dhz}^* + F_{Dez}^*\right) - \frac{4}{3}\pi a^3(\rho_p - \rho_f)g$$
$$- V_s(\rho_s - \rho_f)g = 0, \tag{17}$$

where V_s is the dry volume of the membrane layer. Note that $V_s \neq 4\pi(b^3 - a^3)/3$. Let $(F_{Ez}^* + F_{Dhz}^* + F_{Dez}^*) = (f_1'U^* + f_2'E^*)$, f_1' and f_2' being respectively the total force in problems 1 and 2. Then the sedimentation velocity is

$$U = \frac{[4\pi a^3(\rho_p - \rho_f)g/3] + V_s(\rho_s - \rho_f)g}{(4\pi\eta a/3)(f_1' - \delta f_2'/\beta)}$$
$$= \frac{c^3[\phi_p(\rho_p - \rho_f) + \phi_s(\rho_s - \rho_f)]g}{\eta a(f_1' - \delta f_2'/\beta)}, \tag{18}$$

where $\phi_p = (a/c)^3$ and $\phi_s = V_s/(4/3)\pi c^3$ are respectively the volume fraction of the rigid core and that of membrane material. For convenience, U is scaled by the sedimentation velocity of an uncharged, rigid sphere in an infinite fluid, U_0 [22]:

$$U_0 = -\frac{2}{9}\frac{a^2(\rho_p - \rho_f)g}{\eta}. \tag{19}$$

Dividing Eq. (18) by this expression gives the scaled sedimentation velocity:

$$\frac{U}{U_0} = -\frac{9}{2}\left[1 + \frac{\phi_s}{\phi_p}\left(\frac{\rho_s - \rho_f}{\rho_p - \rho_f}\right)\right]\left(f_1' - \frac{\delta}{\beta}f_2'\right)^{-1}. \tag{20}$$

3. Results and discussion

The governing equations and the associated boundary conditions are solved by a pseudo-spectral method based on Chebyshev polynomials, which is found to be accurate and efficient for solving electrokinetic phenomena of the present type [20]. The influences of the key parameters of the system under consideration on the sedimentation potential and sedimentation velocity are examined through numerical simulation. These include the scaled thickness of double layer $(\kappa a)^{-1}$, the scaled surface potential on the rigid core of a particle ϕ_r, and the amount of fixed charge in the membrane layer of a particle $Q_{\mathrm{fix}} = (\rho_{\mathrm{fix}}a^2/\varepsilon\zeta_a)$. For illustration, an aqueous KCl solution is considered; other types of electrolytes can be treated in a similar manner. The values of physical quantities assumed are $T = 298.15$ K, $\varepsilon = 8.854 \times 10^{-12} \times 78.54688$ F/m, $\eta_0 = 0.8904$ cp, $\rho_f = 0.99704$ g/cm^3, $\rho_p = \rho_s = 1.05$ g/cm^3, $Z_1 = Z_{\mathrm{K}^+} = 1$, $Z_2 = Z_{\mathrm{Cl}^-} = -1$, $D_1 = D_{\mathrm{K}^+} = 1.962297 \times 10^{-5}$ cm^2/s, $D_2 = D_{\mathrm{Cl}^-} = 2.037051 \times 10^{-5}$ cm^2/s. Also, we choose $\lambda a = 10$, $H = 0.421875$, $d/a = 0.5$, and $\mathrm{Pe}_1 = \mathrm{Pe}_2 = 0.01$.

3.1. Influence of κa

Figs. 2a, 3a, and 4a show the variations of the scaled sedimentation potential E^*/U^* as a function of κa at various values of Q_{fix}, and the corresponding variations in the scaled sedimentation velocity U/U_0 are presented in Figs. 2b, 3b, and 4b. Features common to E^*/U^* are that it approaches a constant value when κa is either very small or very large, and it has a local maximum if ϕ_r is sufficiently high. These features are similar to those for rigid spheres [20]. Fig. 4a reveals that for $Q_{\mathrm{fix}} = 10$, E^*/U^* may also have a local minimum. The behaviors of E^*/U^* observed in Figs. 2a, 3a, and 4a can be explained as follows. According to its definition, $E^*/U^* = -\delta/\beta$, where δ and β are respectively the net currents across the plane $\theta = \pi/2$ in problems 1 and 2. Equation (8) indicates that the current $I_\theta(r^*)$ comprises the current arising from the flow of the liquid phase, $I_{\theta,c}$, and arising from the diffusion of ionic species, $I_{\theta,d}$; that is,

$$I_\theta = I_{\theta,c} + I_{\theta,d}, \tag{21}$$

$$I_{\theta,c} = \left[\exp\left(-\phi_r\phi_1^*\right) - \exp\left(\alpha\phi_r\phi_1^*\right)\right]\frac{\mathrm{d}\Psi}{\mathrm{d}r^*}, \tag{22}$$

$$I_{\theta,d} = -\frac{1}{\phi_r}\left[\frac{1}{\mathrm{Pe}_1}\exp\left(-\phi_r\phi_1^*\right)\right.$$
$$\left. + G_1^*\frac{\alpha}{\mathrm{Pe}_2}\exp\left(\alpha\phi_r\phi_1^*\right)G_2^*\right]. \tag{23}$$

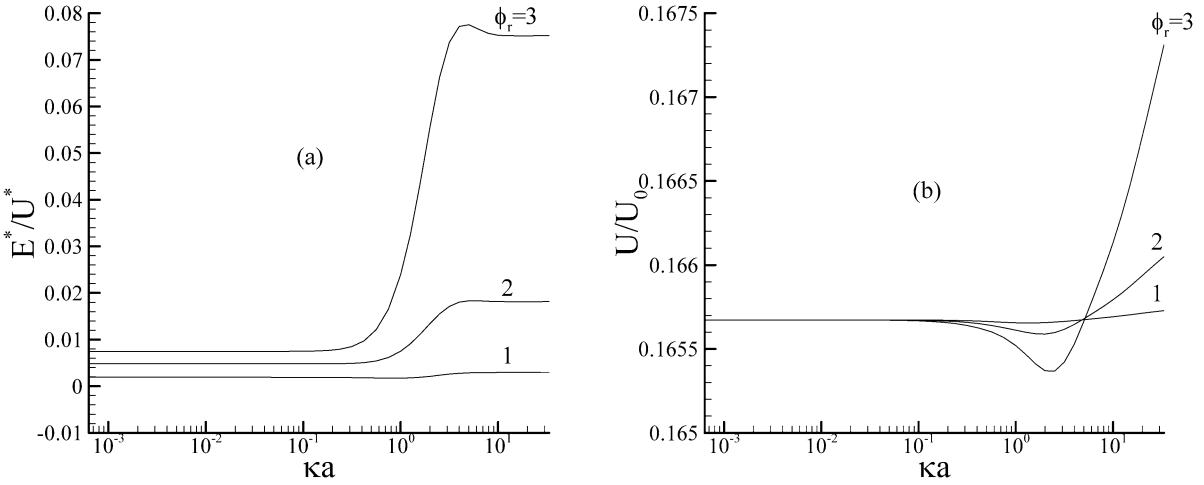

Fig. 2. Variation of scaled sedimentation potential E^*/U^* (a) and scaled sedimentation velocity U/U_0 (b) as a function of κa at various ϕ_r for $Q_{\text{fix}} = 0$.

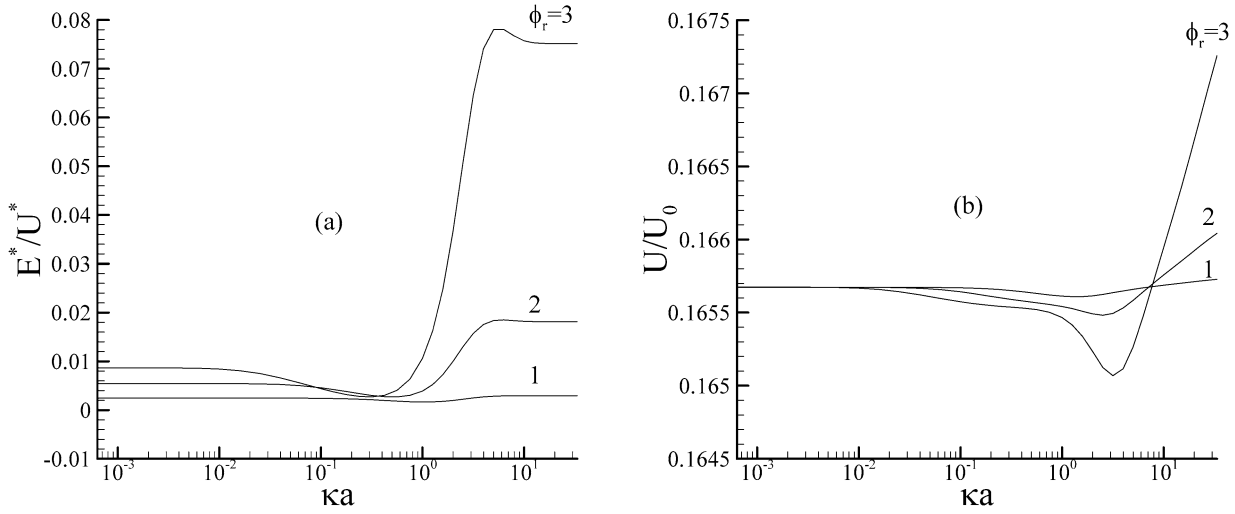

Fig. 3. Variation of scaled sedimentation potential E^*/U^* (a) and scaled sedimentation velocity U/U_0 (b) as a function of κa at various ϕ_r for $Q_{\text{fix}} = 10$.

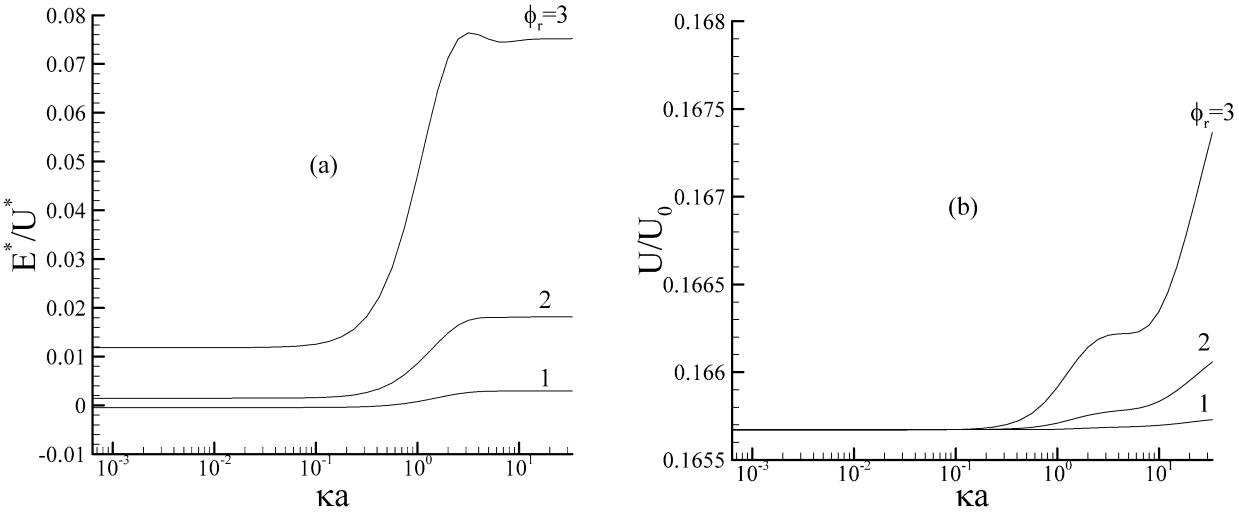

Fig. 4. Variation of scaled sedimentation potential E^*/U^* (a) and scaled sedimentation velocity U/U_0 (b) as a function of κa at various ϕ_r for $Q_{\text{fix}} = -10$.

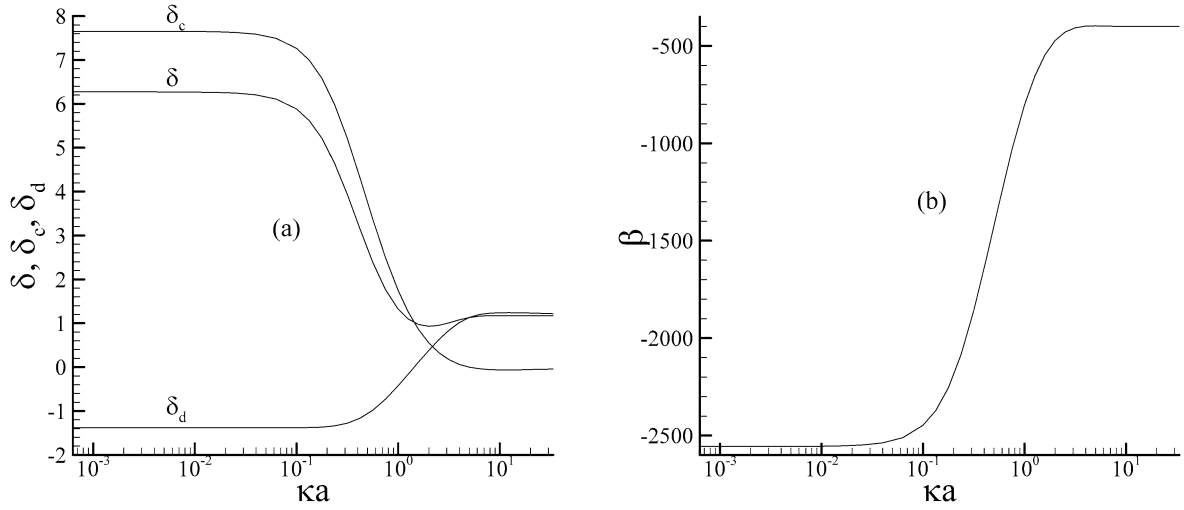

Fig. 5. Variation of net current as a function of κa for $\phi_r = 1.0$ and $Q_{\text{fix}} = 10$. (a) Problem 1; (b) problem 2.

We define

$$\delta_c \equiv \left(\int_1^{c/a} I_{\theta,c}\, \mathrm{d}r^* \right)_{\text{problem 1}}, \tag{24}$$

$$\delta_d \equiv \left(\int_1^{c/a} I_{\theta,d}\, \mathrm{d}r^* \right)_{\text{problem 1}}, \tag{25}$$

$$\beta_c \equiv \left(\int_1^{c/a} I_{\theta,c}\, \mathrm{d}r^* \right)_{\text{problem 2}}, \tag{26}$$

$$\beta_d \equiv \left(\int_1^{c/a} I_{\theta,d}\, \mathrm{d}r^* \right)_{\text{problem 2}}, \tag{27}$$

$$\delta = \delta_c + \delta_d, \tag{28}$$

$$\beta = \beta_c + \beta_d. \tag{29}$$

The variations of δ, δ_c, δ_d, and β as a function of κa at two levels of ϕ_r are illustrated in Figs. 5 and 6. Figs. 5a and 6a show the currents in problem 1, where particles sediment in the absence of an induced electric field. These figures suggest that δ_c, the current arising from the flow of the liquid phase, approaches a constant value as $\kappa a \to 0$ and approaches zero as $\kappa a \to \infty$. For medium values of κa, it decreases with the increase in κa. In contrast, for medium values of κa, the current arising from the diffusion of ionic species, δ_d, increases with the increase in κa; it approaches to a constant value as $\kappa a \to 0$, and to another constant value as $\kappa a \to \infty$. This is because if κa is sufficiently small, the double layer surrounding a particle is thick enough to exceed the boundary of a cell, which implies that the distribution of ionic species in the system is essentially uniform. In this case, the distribution of ionic species is insensible to the variation of κa, so are δ_c and δ_d. Note that although the driving force for ionic diffusion is negligible in this case, because the membrane layer of a particle carries fixed charge, the migration of ionic species due to the presence of the associated electric field still occurs and, therefore, δ_d does not approach zero. As κa increases to an extent such that the corresponding double layer becomes thinner than the radius of a cell, the gradient of ionic concentration increases, so is the driving force for ionic diffusion and, therefore, δ_d increases. On the other hand, if κa is large, because double layer is thin, ionic species are close to particle surface and the liquid outside the double layer is close to electroneutrality. Since the flow of liquid occurs mainly outside the double layer, the current arising from the flow of liquid phase is small, so is δ_c. If $\kappa a \to \infty$, the double layer is infinitely thin, the flow of the liquid phase yields essentially no current and $\delta_c \to 0$. Since $\delta = \delta_c + \delta_d$, when κa is small, the current is mainly contributed by the flow of the liquid phase, and it is mainly contributed by the diffusion of ionic species when κa is large. For an intermediate value of κa, the behavior of δ is determined by the sum of the two competing factors. The general trends of the currents in problem 2, are similar to those of problem 1, shown in Figs. 5a and 6a. Here, because particle remains fixed, the flow of liquid is relatively slow, and the corresponding current β_c almost vanishes. Since the current is contributed mainly by the diffusion of ionic species, the curve of β almost coincide with that of β_d. The behaviors of E^*/U^* observed in Figs. 2a, 3a, and 4a are the net results of the simultaneous variations in δ and β.

As illustrated in Fig. 2b, for the case when the membrane layer of a particle is free of fixed charge, if κa is sufficiently small, the overlapping between neighboring double layers is significant, which has the effect of retarding the sedimentation of particles. Also, because the distribution of ionic species is rather uniform and almost uninfluenced by the induced electric field, therefore U/U_0 remains at a constant value. As κa increases up to abut 0.1, the distortion of the double layer surrounding a particle becomes significant, yielding an induced electric field which is in the opposite direction as that of its sedimentation. When this occurs, the

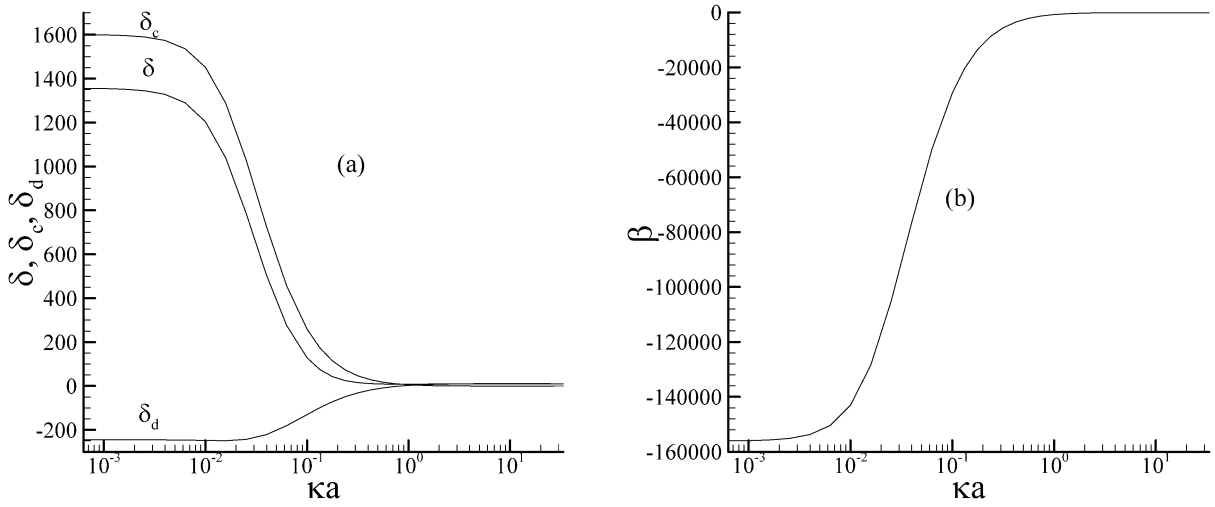

Fig. 6. Variation of net current as a function of κa for $\phi_r = 3.0$ and $Q_{\text{fix}} = 10$. (a) Problem 1; (b) problem 2.

sedimentation is retarded, the so-called polarization or relaxation effect. Furthermore, if the double layer is thinner than the outer boundary of the membrane layer of a particle, because the fluid flow in the membrane layer becomes important, the hydrodynamic retardation increases accordingly and the sedimentation of the particle is slowed down. However, if κa is sufficiently large, the electric gradient near the particle $\nabla\phi_1$ becomes significant. The corresponding electric field, the so-called internal electric field, has the effect of inhibiting double layer deformation, thereby reducing the effect of double layer polarization. The influence of the internal electric field starts to dominate if κa is increased further. Also, because both the overlapping between neighboring double layers and the hydrodynamic retardation due to fluid flow in the membrane layer are unimportant, U/U_0 increases with κa. This is why U/U_0 shows a local minimum as κa varies. Note that although only the results for $\kappa a < 20$ are presented, it can be expected that the sedimentation velocity will approach a constant value when κa is sufficiently large. It is interesting to note that a reversal relation between U/U_0 and ϕ_r is present in Fig. 2b, where for κa smaller than $\approx$5, the larger the value of ϕ_r the smaller the value of U/U_0, but the reverse is true if κa exceeds $\approx$5. This can be explained by the fact that when the effect of double-layer polarization is important, the higher the surface potential the stronger the induced electric field, which is in the opposite direction as that of sedimentation, and the slower the sedimentation velocity. On the other hand, the higher the surface potential the greater the corresponding electric gradient, and more the phenomenon of double-layer polarization is inhibited, and the faster the rate of increase in U/U_0. The general behaviors of U/U_0 shown in Fig. 3b for the case when the membrane layer of a particle is positively charged are similar to those for the case when it is free of fixed charge. The decrease of U/U_0 near $\kappa a = 0.01$ arises from the effect of double-layer polarization. The reversal relation between U/U_0 and ϕ_r observed in Fig. 2b is also present except that it occurs at a larger κa ($\cong 10$). In Fig. 4b, because the sign of the fixed charge in the membrane layer of a particle is different from that on its rigid core, the general trends of U/U_0 becomes different from that in Figs. 2b and 3b. However, they can be explained by similar reasoning. Note that while the double-layer polarization associated with a positively charged core surface of a particle has the effect of retarding its sedimentation that associated with its negatively charged membrane layer has the effect of accelerating its sedimentation. Under the conditions assumed in Fig. 4b, the latter is more important than the former and, therefore, the local minimum of U/U_0 does not appear. The occurrence of an inflection point in Fig. 4b for the case when ϕ_r is sufficiently high is a net result of the competition of double-layer polarization, internal electric field, and hydrodynamic retardation of membrane layer. Note that for the present case, because double-layer polarization is advantageous to the sedimentation of a particle, the higher the level of ϕ_r the larger the U/U_0, which is different from that observed in Figs. 2b and 3b.

3.2. *Influence of ϕ_r*

Figs. 7–9 illustrate the variations of U/U_0 as a function of ϕ_r for various combinations of κa and Q_{fix}. Fig. 7 shows that if the membrane layer of a particle is free of fixed charge, U/U_0 is insensitive to the variation of ϕ_r when $\kappa a = 0.1$. As mentioned previously, this is because if double layer is thick, the distribution of ionic species is uniform and the influence of surface potential on the sedimentation velocity is unimportant. At $\kappa a = 1.0$, U/U_0 decreases monotonically with the increase in ϕ_r. Referring to the discussion of Fig. 2b, this arises from the influence of double-layer polarization, which is more significant at a higher level of ϕ_r. If $\kappa a = 10$, then U/U_0 increases monotonically with the increase in ϕ_r. Referring to the discussion of Fig. 2b, this is because if double layer is sufficiently thin, double-layer polarization is inhibited by the electric potential gradient near particle surface, which increases with the increase in ϕ_r. The

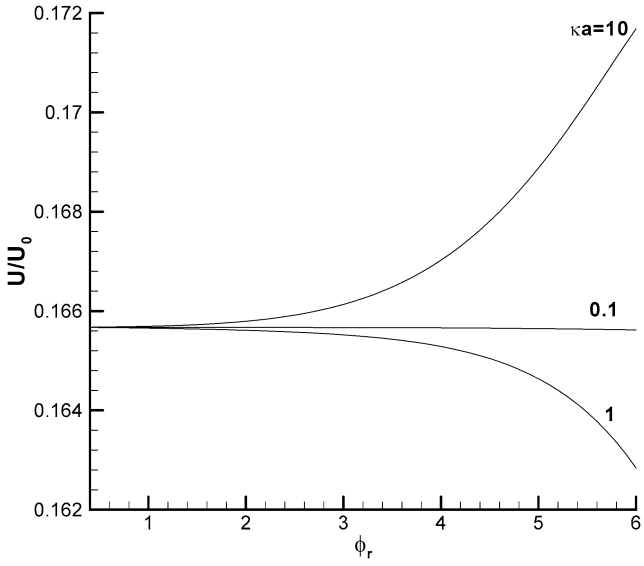

Fig. 7. Variation of scaled sedimentation velocity U/U_0 as a function of scaled surface potential ϕ_r at various κa for $Q_{\text{fix}} = 0$.

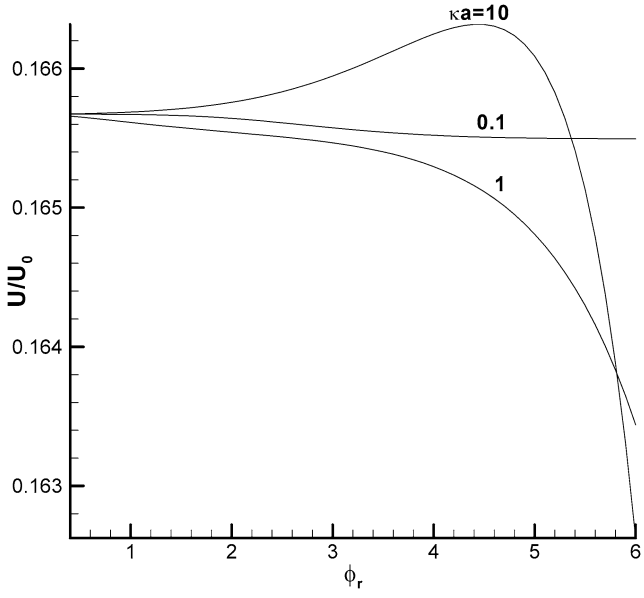

Fig. 8. Variation of scaled sedimentation velocity U/U_0 as a function of scaled surface potential ϕ_r at various κa for the case when $Q_{\text{fix}} = 10$.

general trends of U/U_0 presented in Fig. 8, where the membrane layer of a particle carries positive fixed charge, are similar to those for the case it is free of fixed charge, except that U/U_0 exhibits a local maximum when $\kappa a = 10$. This is because the presence of the positive fixed charge makes the effect of double-layer polarization more important, and a greater electric potential gradient is necessary to compete with that effect. As mentioned in the discussion of Fig. 3b, the value of κa at which the reversal relation between U/U_0 and ϕ_r occurs is larger than that for the case when the membrane layer is free of fixed charge. According to Fig. 3b, the former occurs at $\kappa a = 10$, that is why U/U_0 has a local maximum when this value of κa. The membrane

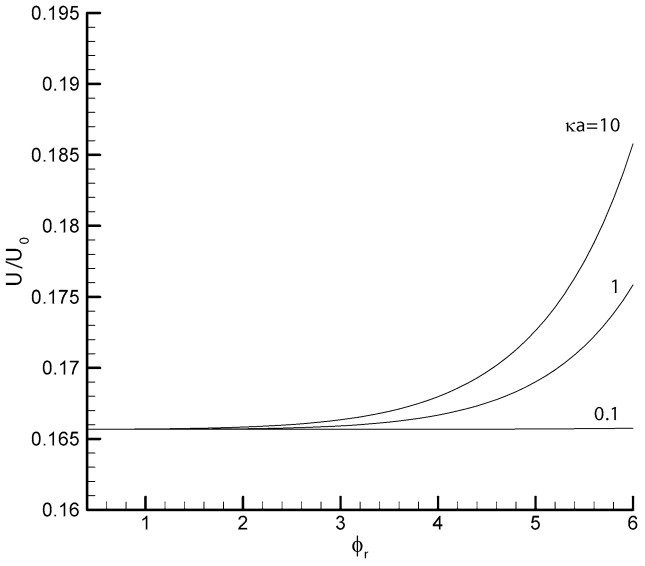

Fig. 9. Variation of scaled sedimentation velocity U/U_0 as a function of scaled surface potential ϕ_r at various κa for $Q_{\text{fix}} = -10$.

layer of a particle carries negative fixed charge in Fig. 9, and we see that, regardless of the value of κa, U/U_0 increases monotonically with the increase in ϕ_r. As mentioned previously, this is because the effect of double-layer polarization is advantageous to the sedimentation of a particle, and the reversal relation between U/U_0 and ϕ_r does not occur.

3.3. *Influence of* Q_{fix}

The variations of E^*/U^* and U/U_0 as a function of κa at various Q_{fix} are summarized in Fig. 10. Fig. 10a indicates that if κa is small, E^*/U^* increases with Q_{fix} when it is positive, and it shifts to a more negative value when Q_{fix} is negative. On the other hand, if κa is large, E^*/U^* becomes insensitive to the variation of Q_{fix}. As discussed previously, for κa in the range $[0.1, 1.0]$, if ϕ_r is low, E^*/U^* has a local minimum. Fig. 10a reveals that this local minimum is influenced both by ϕ_r and by the charged conditions of the membrane layer of a particle; depending upon the amount of fixed charge and its sign, the local minimum may either pronounced or disappear. As can be seen in Fig. 10b, for κa in the range $[0.1, 1.0]$, where the effect of double-layer polarization is significant, a positive Q_{fix} will decelerate the sedimentation of a particle, but a negative Q_{fix} will accelerate its sedimentation. For both $Q_{\text{fix}} = -5$ and -10 the influence of double-layer polarization appears to be unimportant. This can be explained by that the electric force arising from the negative fixed charge in the membrane layer of a particle is roughly balanced by that arising from the positive charge on its rigid core. Note that it is not always true that a negative Q_{fix} is advantageous to the sedimentation of a particle, and the sedimentation velocity is not always increases with the amount of negative fixed charge. For instance, as illustrated in Fig. 11, if $\kappa a = 1.0$, U/U_0 reaches a maximal value when $Q_{\text{fix}} \cong -10$; a more negative Q_{fix} leads to

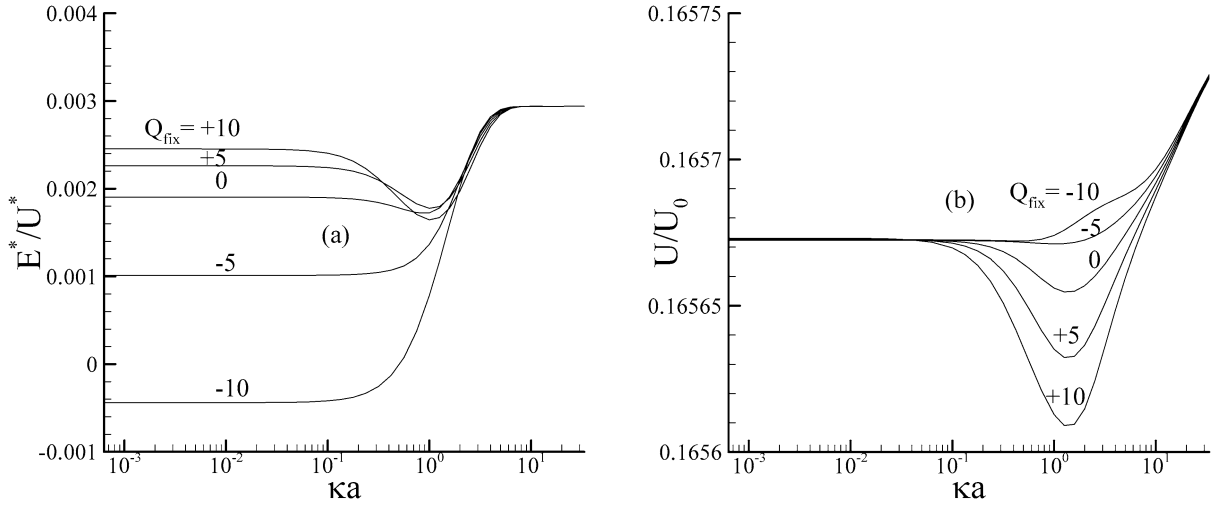

Fig. 10. Variation of scaled sedimentation potential E^*/U^* (a) and scaled sedimentation velocity U/U_0 (b) as a function of κa at various Q_{fix} for $\phi_r = 1.0$.

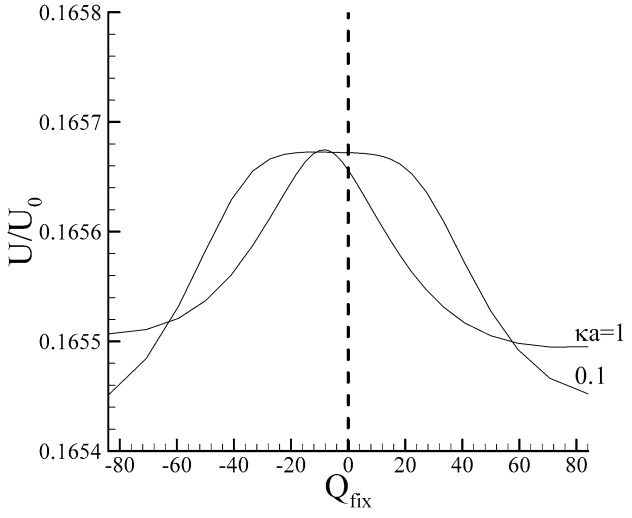

Fig. 11. Variation of scaled sedimentation velocity U/U_0 as a function of Q_{fix} at different κa for $\phi_r = 1.0$.

a smaller U/U_0. This is because of the fact that when the negative fixed charge in the membrane layer of a particle exceeds a certain amount, the positive charge on the surface of its rigid core becomes relatively unimportant. In this case, the effect of double-layer polarization is dominated by the fixed charge and, because the direction of the corresponding induced electric field is in the z-direction, the more the amount of fixed charge the greater the corresponding electric force is and the slower is the sedimentation velocity.

3.4. Influence of H

The influence of the concentration of particles, measured by H, on the sedimentation velocity and sedimentation potential are illustrated in Figs. 12 and 13, respectively. The former reveals that U/U_0 decreases with H. This is expected because the higher the concentration of particles the more significant the overlapping of the neighboring double layers, which leads to a greater hydrodynamic resistance for liquid flow. The dependence of E^*/U^* on H, however, depends on both κa and ϕ_r as illustrated in Fig. 13. Fig. 13a indicates that for the case when the surface potential is low, regardless of the value of κa, the higher the concentration of particles the higher the sedimentation potential. If the surface potential is sufficiently high, then E^*/U^* increases with H when κa is very small or vary large, and the reverse is true if κa takes a medium value, as shown in Fig. 13b. These behaviors can be explained as follows. When ϕ_r is low, the effect of double-layer polarization is insignificant. In this case if H is high, the concentration of ionic species near a particle is relatively higher than that for the case when it is low and, therefore, the corresponding E^*/U^* is higher. On the other hand, if ϕ_r is high, the effect of double-layer polarization needs to be considered. However, if double-layer is very thick, since the overlapping between neighbor double layers is serious, the effect of double-layer polarization is shielded. For a medium thick double layer, again, due to the possible interaction between neighboring double layers, the higher the concentration of particles the less significant the effect of double layer, and therefore the lower the sedimentation potential. If the double layer is very thin, similarly to the case when ϕ_r is low, the higher the concentration of particles, the higher the concentration of ionic species near a particle, and therefore, the higher the corresponding sedimentation potential. In general, the influence of the concentration of particles on the sedimentation potential is similar to that for the case of rigid particles [11,23].

In summary, the sedimentation of a concentrated dispersion of composite spherical particles, which simulate biocolloids such as microorganisms and cells, and particles covered by a membrane layer, is modeled theoretically. The influences of the thickness of double layer, the surface potential on the rigid core of a particle, and the amount of fixed charge in its membrane layer on the sedimentation potential and sedimentation velocity are examined through numerical simulation. For the case when the rigid core of a particle is

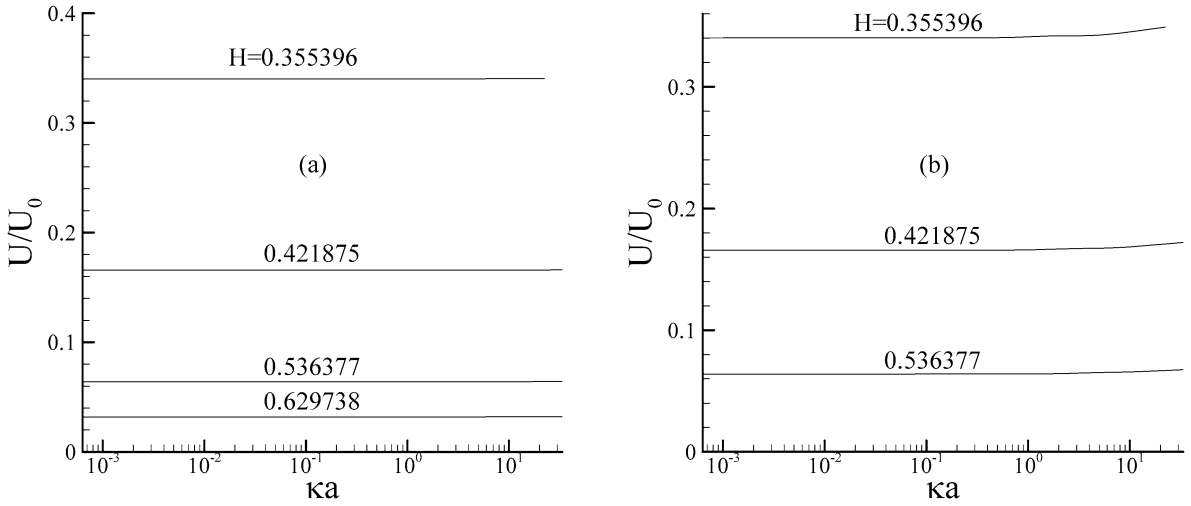

Fig. 12. Variation of scaled sedimentation velocity U/U_0 as a function of κa at various H when $\phi_r = 1.0$ (a) and $\phi_r = 3.0$ (b) for $Q_{\text{fix}} = 0$, $\lambda a = 10$, $d/a = 0.5$, and $\text{Pe}_1 = \text{Pe}_2 = 0.01$.

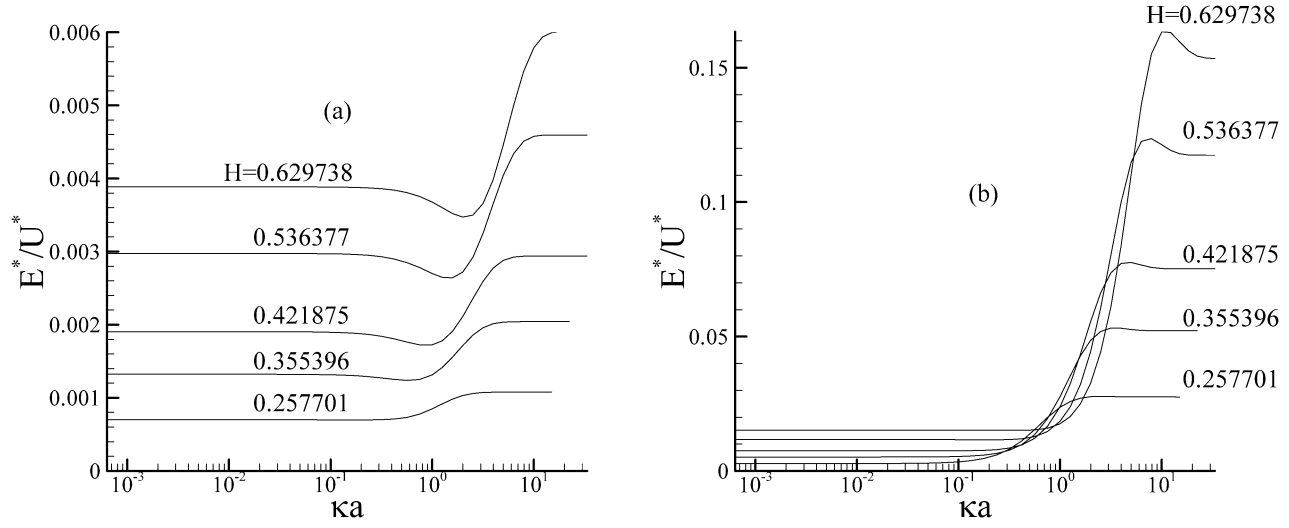

Fig. 13. Variation of scaled sedimentation potential E^*/U^* as a function of κa at various H when $\phi_r = 1.0$ (a) and $\phi_r = 3.0$ (b) for $Q_{\text{fix}} = 0$, $\lambda a = 10$, $d/a = 0.5$, and $\text{Pe}_1 = \text{Pe}_2 = 0.01$.

positively charged, the results of numerical simulation can be summarized as follows:

(1) If the surface potential on the rigid core of a particle is sufficiently high and the membrane layer is either free of fixed charge or carries negative charge, the sedimentation potential has a local maximum as the thickness of double layer varies. It can have both a local maximum and a local minimum if the membrane layer carries positive fixed charge.

(2) If the membrane layer is either free of fixed charge or carries positive fixed charge, the sedimentation velocity shows a local minimum as the thickness of double layer varies, which arises mainly from the effect of double-layer polarization. For a thick double layer, the sedimentation velocity decreases with the increase in the surface potential on the rigid core of a particle, but the reverse is true if it becomes thin. The local minimum in the sedimentation velocity does not show if the membrane layer carries negative fixed charge, and the higher the surface potential on the rigid core of a particle the faster the sedimentation velocity is.

(3) If the membrane layer of a particle is free of fixed charge, the sedimentation velocity is insensitive to the variation of the surface potential on the rigid core of a particle when double layer is thick. The sedimentation velocity decreases monotonically with the increase in the surface potential when the thickness of double layer is on the order of the radius of the rigid core of a particle, and the reverse is true if it is sufficiently thin. If the membrane layer of a particle carries positive fixed charge and the double layer is sufficiently thin, the sedimentation velocity has a local maximum as the surface potential varies. If the membrane layer of a particle carries negative fixed charge, regardless of the thickness of double layer, the sedimentation velocity increases monoton-

ically with the increase in the surface potential on the rigid core of a particle.

(4) If double layer is thick, the sedimentation potential increases with the amount of positive fixed charge, and it shifts to a more negative value when the fixed charge is negative. On the other hand, if double layer is thin, the sedimentation potential becomes insensitive to the variation of the amount of fixed charge. For a medium thick double layer if the surface potential is low, the sedimentation potential has a local minimum. This local minimum is influenced both by the surface potential and by the charged conditions of the membrane layer; depending upon the amount of fixed charge and its sign, the local minimum may either pronounced or disappear. It is not always true that negative fixed charge is advantageous to the sedimentation of a particle, and the sedimentation velocity is not always increases with the amount of negative fixed charge.

(5) The sedimentation potential increases with the concentration of particles. The relation between the sedimentation velocity and the concentration of particles, however, depends on the thickness of double layer. If the double layer is thick, the higher the concentration of particles the faster the sedimentation velocity, but the reverse is true if it is thin.

Acknowledgment

This work is supported by the National Science Council of the Republic of China.

Appendix A

The scaled equations and the associated boundary conditions for the electric, the flow, and the concentration fields are summarized as follows [18]:

$$\nabla^{*2}\phi_1^* = -\frac{(\kappa a)^2}{(1+\alpha)\phi_r}\left[\exp\left(-\phi_r\phi_1^*\right) - \exp\left(\alpha\phi_r\phi_1^*\right)\right] - Q_{\text{fix}}, \quad a < r < b, \tag{A.1}$$

$$\nabla^{*2}\phi_1^* = -\frac{(\kappa a)^2}{(1+\alpha)\phi_r}\left[\exp\left(-\phi_r\phi_1^*\right) - \exp\left(\alpha\phi_r\phi_1^*\right)\right], \quad b < r < c, \tag{A.2}$$

$$L^2\Phi_2 - \frac{(\kappa a)^2}{(1+\alpha)}\left[\exp\left(-\phi_r\phi_1^*\right) + \alpha\exp\left(\alpha\phi_r\phi_1^*\right)\right]\Phi_2 = \frac{(\kappa a)^2}{(1+\alpha)}\left[\exp\left(-\phi_r\phi_1^*\right)G_1 + \alpha\exp\left(\alpha\phi_r\phi_1^*\right)G_2\right], \tag{A.3}$$

$$L^2G_1 - \phi_r^2\frac{\mathrm{d}\phi_1^*}{\mathrm{d}r^*} = \mathrm{Pe}_1\,\phi_r^2 v_r^*\frac{\mathrm{d}\phi_1^*}{\mathrm{d}r^*}, \tag{A.4}$$

$$L^2G_2 + \alpha\phi_r^2\frac{\mathrm{d}\phi_1^*}{\mathrm{d}r^*} = \mathrm{Pe}_2\,\phi_r^2 v_r^*\frac{\mathrm{d}\phi_1^*}{\mathrm{d}r^*}, \tag{A.5}$$

$$D^4\Psi - (\lambda a)^2 D^2\Psi = -\frac{(\kappa a)^2}{1+\alpha}\left[\left(n_1^*G_1 + n_2^*G_2\right)\frac{\mathrm{d}\phi_1^*}{\mathrm{d}r^*}\right], \quad a < r < b, \tag{A.6}$$

$$D^4\Psi = -\frac{(\kappa a)^2}{1+\alpha}\left[\left(n_1^*G_1 + n_2^*G_2\right)\frac{\mathrm{d}\phi_1^*}{\mathrm{d}r^*}\right], \quad b < r < c. \tag{A.7}$$

In these expressions, $Q_{\text{fix}} = \rho_{\text{fix}}a^2/\varepsilon\zeta_a$ is the scaled total amount of fixed charge, $\phi_r = z_1 e\zeta_a/kT$ is the scaled surface potential of particle, $\kappa^{-1} = [\varepsilon kT/\sum n_{j0}(ez_j)^2]^{1/2}$ is the Debye length, $\mathrm{Pe}_j = U_E a/D_j$, $j = 1, 2$, is the electric Peclet number of ionic species j, α is the minus value of the ratio of the valence of anion to the valence of cations, and $(\lambda a)^2 = (\gamma a^2/\eta)$ is the dimensionless group for the friction coefficient of the membrane layer. The linear operators L^2 and D^4 are defined respectively by

$$L^2 \equiv \frac{\mathrm{d}^2}{\mathrm{d}r^{*2}} + \frac{2}{r^*}\frac{\mathrm{d}}{\mathrm{d}r^*} - \frac{2}{r^{*2}} \tag{A.8}$$

and

$$D^4 = D^2D^2 = \left(\frac{\mathrm{d}^2}{\mathrm{d}r^{*2}} - \frac{2}{r^{*2}}\right)^2. \tag{A.9}$$

The associated boundary conditions are

$$\frac{\mathrm{d}\Phi_2}{\mathrm{d}r^*} = 0, \quad r^* = 1, \tag{A.10}$$

$$\Phi_2|_{r^*=b^-/a} = \Phi_2|_{r^*=b^+/a}, \quad r^* = \frac{b}{a}, \tag{A.11}$$

$$\left.\frac{\mathrm{d}\Phi_2}{\mathrm{d}r^*}\right|_{r^*=b^-/a} = \left.\frac{\mathrm{d}\Phi_2}{\mathrm{d}r^*}\right|_{r^*=b^+/a}, \quad r^* = \frac{b}{a}, \tag{A.12}$$

$$\frac{\mathrm{d}\Phi_2}{\mathrm{d}r^*} = -E_z^*, \quad r^* = \frac{c}{a}, \tag{A.13}$$

$$\frac{\mathrm{d}G_j}{\mathrm{d}r^*} = 0, \quad r^* = 1, \quad j = 1, 2, \tag{A.14}$$

$$G_j|_{r^*=b^-/a} = G_j|_{r^*=b^+/a}, \quad r^* = \frac{b}{a}, \quad j = 1, 2, \tag{A.15}$$

$$\left.\frac{\mathrm{d}G_j}{\mathrm{d}r^*}\right|_{r^*=b^-/a} = \left.\frac{dG_j}{\mathrm{d}r^*}\right|_{r=b^+/a}, \quad r^* = \frac{b}{a}, \quad j = 1, 2, \tag{A.16}$$

$$G_1 = -\Phi_2 \quad \text{and} \quad G_2 = -\Phi_2, \quad r^* = \frac{c}{a}, \tag{A.17}$$

$$\Psi^* = -\frac{1}{2}r^{*2}U^* \quad \text{and} \quad \frac{\mathrm{d}\Psi^*}{\mathrm{d}r^*} = -r^*U^*, \quad r^* = 1, \tag{A.18}$$

$$\Psi^*|_{r^*=b^-/a} = \Psi^*|_{r^*=b^+/a} \quad \text{and}$$

$$\left.\frac{\mathrm{d}\Psi^*}{\mathrm{d}r^*}\right|_{r^*=b^-/a} = \left.\frac{d\Psi^*}{\mathrm{d}r^*}\right|_{r^*=b^+/a}, \quad r^* = \frac{b}{a}, \tag{A.19}$$

$$\left.\frac{\mathrm{d}^2\Psi^*}{\mathrm{d}r^{*2}}\right|_{r^*=b^-/a} = \left.\frac{d^2\Psi^*}{\mathrm{d}r^{*2}}\right|_{r^*=b^+/a}, \quad r^* = \frac{b}{a}, \tag{A.20}$$

$$\left[\frac{\mathrm{d}^3\Psi^*}{\mathrm{d}r^{*3}} - (\lambda a)^2\frac{\mathrm{d}\Psi^*}{\mathrm{d}r^*}\right]_{r^*=b^-/a} = \left[\frac{\mathrm{d}^3\Psi^*}{\mathrm{d}r^{*3}}\right]_{r^*=b^+/a}, \quad r^* = \frac{b}{a}, \tag{A.21}$$

$$\Psi^* = 0 \quad \text{and} \quad \left(\frac{\mathrm{d}^2}{\mathrm{d}r^{*2}} - \frac{2}{r^{*2}}\right)\Psi^* = 0, \quad r^* = \frac{c}{a}. \tag{A.22}$$

In these expressions, $\phi_1^*(r^*) = \phi_1(r)/\zeta_a$ is the scaled equilibrium potential, $\Phi_2(r^*) = \phi_2(r,\theta)/\zeta_a\cos\theta$ is the scaled

perturbed potential arising from the perturbation of the applied electric field, $G_j(r^*) = g_j(r,\theta)/\zeta_a \cos\theta$ is the scaled perturbed potential for ionic species j arising from the perturbation of the flow field, and $\Psi^*(r^*) = \psi(r,\theta)/U_0 a^2 \sin^2\theta$ is the scaled stream function.

References

[1] M. Smoluchowski, in: L. Graetz (Ed.), Handbuch der Elecktrizitat und des Magnetismus, vol. II, Barth, Leipzig, 1921.
[2] F. Booth, J. Chem. Phys. 22 (1954) 1956.
[3] F. Booth, Proc. R. Soc. London Ser. A 203 (1950) 514.
[4] J.Th.G. Overbeek, Kolloid-Beih. 54 (1943) 287.
[5] D.A. Saville, Adv. Colloid Interface Sci. 16 (1982) 267.
[6] H. Ohshima, T.W. Healy, L.R. White, R.W. O'Brien, J. Chem. Soc. Faraday Trans. 2 80 (1984) 1299.
[7] S.R. de Groot, P. Mazur, J.Th.G. Overbeek, J. Chem. Phys. 20 (1952) 1825.
[8] S. Levine, G.H. Neale, N. Epstein, J. Colloid Interface Sci. 57 (1976) 421.
[9] H. Ohshima, J. Colloid Interface Sci. 208 (1998) 295.
[10] E. Lee, J.W. Chu, J.P. Hsu, J. Chem. Phys. 110 (1999) 11643.
[11] M.H. Tse, E. Lee, J.P. Hsu, Langmuir 16 (2000) 1650.
[12] E. Lee, T.S. Tong, M.H. Chih, J.P. Hsu, J. Colloid Interface Sci. 251 (2002) 109.
[13] S. Kuwabara, J. Phys. Soc. Jpn. 14 (1959) 527.
[14] H.J. Keh, Y.C. Liu, J. Colloid Interface Sci. 195 (1997) 169.
[15] H. Ohshima, J. Colloid Interface Sci. 229 (2000) 140.
[16] D.A. Saville, J. Colloid Interface Sci. 222 (2000) 137.
[17] D.A. Saville, J. Colloid Interface Sci. 258 (2003) 56.
[18] E. Lee, K.T. Chou, J.P. Hsu, J. Colloid Interface Sci. 127 (2005) 497.
[19] E. Lee, J.W. Chu, J.P. Hsu, J. Colloid Interface Sci. 205 (1998) 65.
[20] E. Lee, J.W. Chu, J.P. Hsu, J. Chem. Phys. 110 (1998) 23.
[21] J. Happel, H. Brenner, Low-Reynolds Number Hydrodynamics, Nijhoff, Boston, 1983.
[22] R.J. Hunter, Foundations of Colloid Science, vols. 1 and 2, Oxford Univ. Press, London, 1989.
[23] E. Lee, M.H. Chih, J.W. Chu, J.P. Hsu, Langmuir 16 (2000) 1650.